



## Ultrafine grained Fe-Cr-Ni austenitic stainless steels by cold rolling and reversion annealing: A review of progress in Iran

*Meysam Naghizadeh, Mohammad Javad Sohrabi, Hamed Mirzadeh\**

*School of Metallurgy and Materials Engineering, College of Engineering, University of Tehran, Tehran, Iran.*

*Received: 5 September 2020; Accepted: 8 October 2020*

*\* Corresponding author email: [hmirzadeh@ut.ac.ir](mailto:hmirzadeh@ut.ac.ir)*

### ABSTRACT

The notable contributions of Iranian scientists in the field of formation and reversion of strain-induced martensite for grain refinement and enhanced mechanical properties of Fe-Cr-Ni austenitic stainless steels are reviewed. Accordingly, the processing of ultrafine grained (UFG) structure via cold rolling and reversion annealing is summarized for AISI 301, 304, 309Si, 316, and 321 stainless steels, as well as their variants. The repetitive and innovative thermomechanical processing routes are introduced as well. The understanding of the stages of annealing (reversion of strain-induced martensite to austenite, primary recrystallization of the retained austenite, and grain growth) and the underlying reversion mechanisms (diffusional-type and martensitic shear-type) constitute the subsequent part of this overview. Finally, the transformation-induced plasticity (TRIP) effect in the reversion-treated metastable austenitic stainless steels is discussed. The present review paper summarizes these achievements with the discussion on the future prospects in this research field.

**Keywords:** *Austenitic stainless steels; Deformation-induced martensitic transformation; Reversion annealing; Ultrafine grained structure; Mechanical properties; TRIP effect.*

### 1. Introduction

The relatively low yield stress of austenitic stainless steels is their main drawback for many potential applications. Grain refinement has been identified as a viable method to enhance their mechanical properties [1-5]. Since these steels do not experience any notable phase transformations during cooling, the severe plastic deformation (SPD) techniques [6,7] and recrystallization processes [8-11] are normally used for this purpose.

The SPD techniques are normally confined to small specimens and the recrystallization processes are not as effective as SPD processes. In response, the advanced processing route of cold working followed by annealing has been devised for

obtaining ultrafine grained (UFG) austenite [12].

Many austenitic stainless steel grades are metastable at room temperature and the austenite phase transforms to strain-induced martensite during cold working. The formation of martensite is highly dependent on the chemical composition, the deformation temperature, grain size, deformation mode, and other factors [13]. During mechanical testing, the formation of martensite is responsible for the enhanced ductility through the transformation-induced plasticity (TRIP) effect [13-19]. The nucleation sites for the  $\alpha'$ -martensite involve the intersections of shear bands, consisting of bundles of overlapping stacking faults,  $\epsilon$ -martensite (where this hexagonal close

packed phase originates from the stacking faults in the face-centered cubic crystal and its growth occurs by the overlapping of the stacking faults on every second {111} plane), and mechanical twins (form when stacking faults overlap on successive {111} planes) [4,20-26]. However, in the UFG structures, martensite forms preferably on austenite grain boundaries [24,27].

The reverse transformation of strain-induced martensite to austenite during annealing is responsible for the formation of UFG structure, as recently reviewed comprehensively and in details by Järvenpää et al. [24] and Sohrabi et al. [2], and discussed in other investigations [28-31]. A schematic of this processing route is shown in Figure 1. Cold deformation results in the elongation of grains and formation of martensite. It is also possible that some deformed retained austenite remain in the microstructure [30-33]. Therefore, besides the reversion of martensite to UFG austenite, the recrystallization of the retained austenite to micron-size austenite should be also considered during annealing. Obtaining an equiaxed microstructure necessitates the recrystallization of the retained austenite, during which the UFG reversed grains might grow significantly. Therefore, for obtaining a marked grain refinement, the availability of great amounts of martensite before reversion annealing is favorable [2,12,34]. This usually necessitates the application of heavy cold reductions (as this is the case in many Iranian works), which negates the usability of this technique in practice. In this regard, low stacking fault energy (SFE) can enhance martensite formation at lower reductions [13]. The volume fraction of  $\alpha'$ -martensite and  $\epsilon_s$  (the strain required for saturation in the amount of martensite) are closely related to SFE and the chemical driving force of austenite to martensite, where it was argued by Behjati et al. [25] that the driving force/SFE ratio plays a key role in martensitic transformation. Promisingly, for instance for a 301LN grade, cold rolling reductions as low as 35% to 52% seemed to result in excellent strength-ductility combinations, even though the grain size refinement was not most efficient and the obtained grain size was not uniform [24,29,33]. Alternatively, a heterogeneous lamella structure was obtained via cold rolling of 316L grade. Annealing treatment resulted in varying fractions of nano-grains, nano-twins, lamellar coarse grains, and recrystallized grains, with an excellent

combination of strength and ductility [35-37].

The formation and reversion of strain-induced martensite for grain refinement and enhanced properties of austenitic stainless steels has been extensively studied in Iran since a pioneering publication by Mirzadeh and Najafizadeh in 2008 [38]. Accordingly, notable contributions in (I) the processing of fine-grained austenitic stainless steels, (II) the understanding of the different stages of reversion annealing and the underlying mechanisms, and (III) TRIP effect have been made by the Iranian scientists. The present review paper aims to summarize these achievements.

## 2. Beginning of reversion research in Iran

The formation and reversion of strain-induced martensite for grain refinement and enhanced properties of austenitic stainless steels was introduced to Iranian scientists by Mirzadeh and Najafizadeh [38-40]. The effect of cold-working temperature, the amount of deformation, the strain rate, and the initial austenite grain size on the volume fraction of strain-induced martensite in AISI 301LN stainless steel was modeled by means of artificial neural networks (ANNs). Accordingly, for a range of processing parameters, the contour lines of martensite volume fraction were determined as shown in Figure 2 [38]. It can be seen in this figure that the martensite content is increased when the amount of deformation is high or the deformation temperature is low. Moreover, by increasing the strain rate and the ASTM austenite grain size number (i.e. finer grain size), the amount of strain-induced martensite reduced. The appropriate grain refining zone with high martensite content for the subsequent annealing treatment can be determined from this model [38]. A similar model

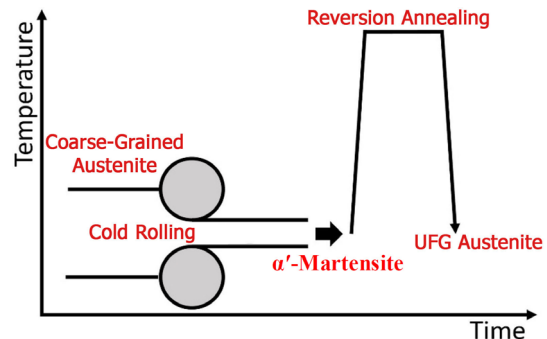


Fig. 1- Schematic of the basic thermomechanical processing route for grain refinement of austenitic stainless steel based on the martensite reversion technique.

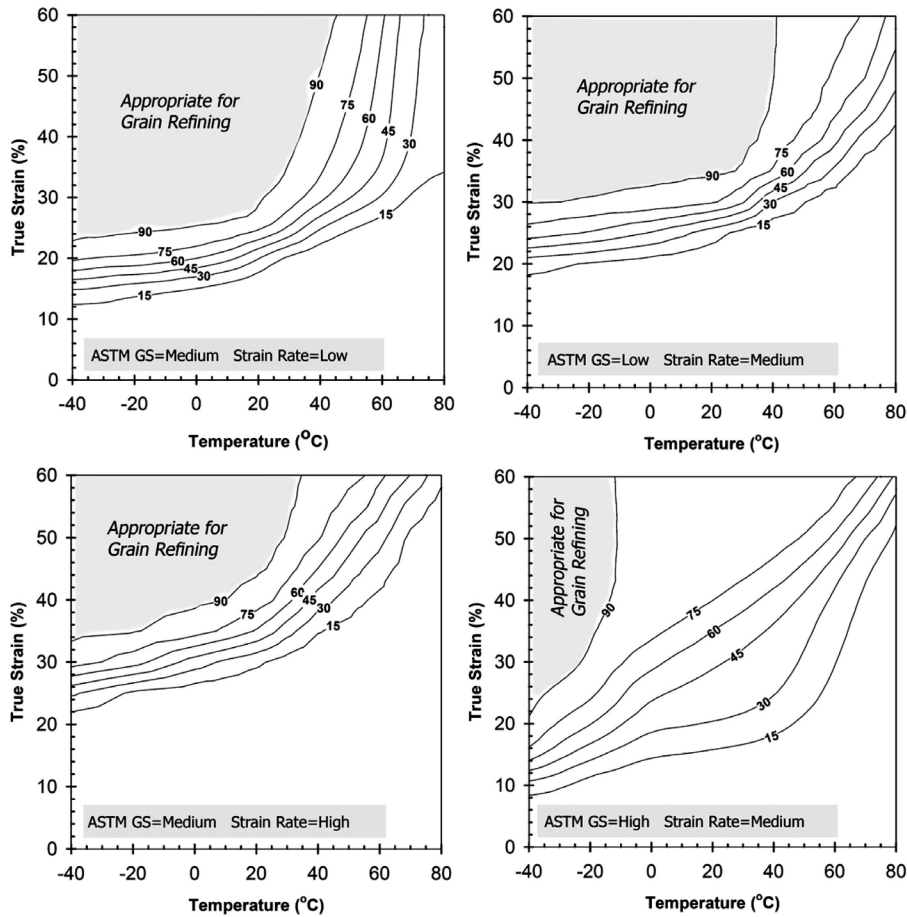


Fig. 2- Contour lines of amount of strain-induced martensite as a function of strain and temperature [38]. The strain rate values were on the order of  $10^{-4}$  and  $10^2 \text{ s}^{-1}$ , which were labeled as low and high, respectively. The ASTM grain size numbers were  $\sim 3$  and  $9$ , which were labeled as low and high, respectively.

was developed for the AISI 304 stainless steel, which can be used as a guide for grain refining that needs high amount of strain-induced martensite or simple cold deformation in which non-magnetic properties are desirable [39]. In contrary to the austenite phase, the strain-induced  $\alpha'$ -martensite phase can be detected by magnetic methods as shown by Shirdel et al. [17].

The effect of annealing temperature and time on the reversion of strain-induced martensite to austenite in the cold worked AISI 304 stainless steel alloy was modeled by means of artificial neural networks and the results are shown in Figure 3 [40]. In this figure, the relative percentage of reverse transformation in the form of  $100 \times (f_{\alpha'}^{initial} - f_{\alpha'}^{reversed}) / f_{\alpha'}^{initial}$  has been shown as the contour lines. The developed model shows that the higher annealing temperature and time may lead to a greater reverted fraction.

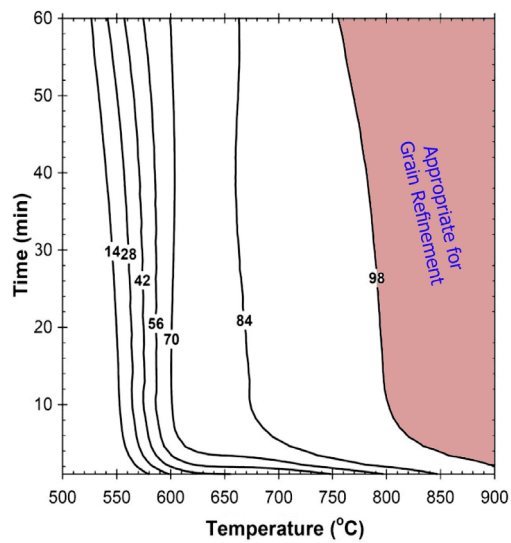


Fig. 3- Contour lines of relative percentage of reverse transformation as a function of annealing conditions [40].

Furthermore, the complete reversion at short times is only achievable by annealing at temperatures higher than  $\sim 750$  °C. This model can be used for determination of appropriate annealing temperature and time for grain refining of austenite to avoid unnecessary long annealing time. Continued annealing, beyond the optimum time, results in the rapid grain growth of the UFG reversed austenite grains [40]. This effect was subsequently confirmed by Naghizadeh and Mirzadeh [41] and Kheiri et al [42]. The introduced concept of relative percentage of reverse transformation, also expressed as the relative reverted fraction, is useful for comparative studies when the initial martensite contents are different [40] and has been subsequently used in more recent studies [31,43].

The success of these research works [38-40], was an impetus for a significant body of research works in the following years, which was realized quickly by several publications on the processing of fine-grained austenitic stainless steels as will be discussed in the following section.

### 3. Processing of fine-grained austenitic stainless steels

Several research groups focused on the processing of fine-grained austenitic stainless steels in Iran. The published research works include a majority of the commercially available Fe-Cr-Ni austenitic stainless steels. However, as preliminary evaluated recently, it is expected that the addition of microalloying elements [44,45] and Mn- and N-containing alloys (with reduced amounts of Ni) [22,46,47] gain more attention in the future.

The martensite reversion process was used by Eskandari et al. [15,48] to obtain nanocrystalline austenitic stainless steels, where for the AISI 301 stainless steel, by decreasing the rolling temperature, the volume fraction of martensite at each strain increased, and  $\epsilon_s$  decreased [48]. In this way, it was possible to obtain a nearly completely martensitic microstructure, consistent with the work of Mirzadeh and Najafzadeh on the AISI 301LN stainless steel [38]. It should be noted that the effect of deformation temperature on the formation of strain-induced martensite and TRIP effect was subsequently studied in detail for the shear punch test (SPT) and uniaxial tensile deformation by Zergani et al. [14,19].

The effect of reversion annealing on the martensite content was studied by Eskandari et al. [48], where a higher temperature resulted in a faster

reversion at shorter holding times. However, in the temperature range of 600 to 850 °C, the highest amount of reverted austenite was  $\sim 95\%$ , which was achievable by annealing at 850 °C for 1 min. This was attributed to the static precipitation of carbides below 1000 °C, which retards the reversion process [48]. The presence of carbides might also locally decrease the martensite start temperature and lead to the formation of martensite during cooling from the annealing temperature [49,50]. This annealing-induced martensite formation was confirmed by Eskandari et al. [48] in an AISI 301 stainless steel, Shirdel et al. [51] in an AISI 304L stainless steel (as shown in Figures 4a for the reversion annealing temperature of 1123 K), and Sadeghpour et al. [45] in an AISI 201L stainless steel. The formation of martensite during annealing might result in the increase of hardness after reversion annealing [52]. This subject has been recently reviewed in details by Sohrabi et al. [2].

Regarding the processing of fine-grained austenitic stainless steels, Forouzan et al. [53]

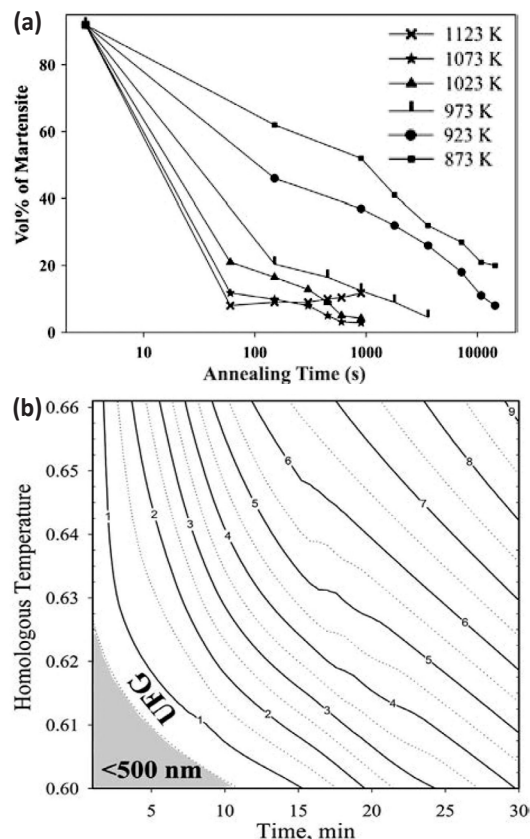


Fig. 4- (a) Progress of reversion during annealing of the cold rolled AISI 304L stainless steel and (b) grain size map (expressed in  $\mu\text{m}$ ) after reversion treatment [51].

summarized the data of the cold rolled and annealed AISI 304L stainless steel in the form of a grain refining diagram as an extension of the idea proposed by Mirzadeh and Najafizadeh [40]. Similarly, the processing of UFG AISI 321 and 321L stainless steels (modified grades with titanium) was studied by Shahri et al. [54] and Rezaei et al. [55], respectively.

Bakhsheshi-Rad et al. [56] studied the grain refinement of AISI 304 stainless steel by the martensite reversion process, where the immersion test showed that the austenitic ultrafine-grained structure exhibits moderate and more uniform pitting corrosion attack compared to the coarser grain in NaCl solution. In an investigation on the effect of surface preparation on the corrosion behavior of AISI 316L stainless steel, Sohrabi et al. [57] showed that the uniform corrosion can be adequately correlated to the surface roughness (Ra), but the pitting resistance was found to mainly relate to the kurtosis (Rku), where by decreasing Rku (increased bluntness of topographic features), the pitting resistance enhanced. It was also found that a surface with Rku less than 3 (platykurtic) is resistant to pitting attack, where this surface can be obtained via electropolishing performed for an optimum time. Sabooni et al. [58] showed that grain refinement (and obtaining the UFG structure by martensite reversion process) significantly improve the corrosion resistance of AISI 304L stainless steel due to the enhanced resistance of the passive layer to pitting attack. Moreover, according

to the results of the dry sliding wear test reported by Nafar Dehsorkhi et al. [59], the UFG steel exhibited better wear resistance under normal loads of 10 N and 20 N, whereas under the normal load of 30 N, it showed weak wear resistance as compared to the steel with larger grain size.

The processing of UFG AISI 304L stainless steel was systematically studied by Shirdel et al. [51], where the evolution of martensite content during annealing is shown in Figures 4a. The grain size map of Figure 4b was also developed by consideration of both reversed grain size and grain growth after the completion of the reversion process. Interestingly, the abnormal grain growth (AGG) was also detected during annealing of the cold rolled sheet [51], which was found to be consistent with the observations of AGG in the coarse-grained counterpart [60,61]. The thermal stability of the UFG structure produced by martensite reversion process was further considered by Sabooni et al [62], where the kinetics of grain growth was studied by the parabolic grain growth formula.

The cold rolling and martensite reversion process has been used on a repetitive basis for more intense grain refinement [63]. This has been studied by Iranian scientists as well, where the usefulness of this processing route has been discussed [47,48,64,65]. It was shown by Naghizadeh and Mirzadeh [65] that while a notable grain refinement can be achieved by the first cycle of this process, the subsequent cycles are considerably less effective (Figure 5).

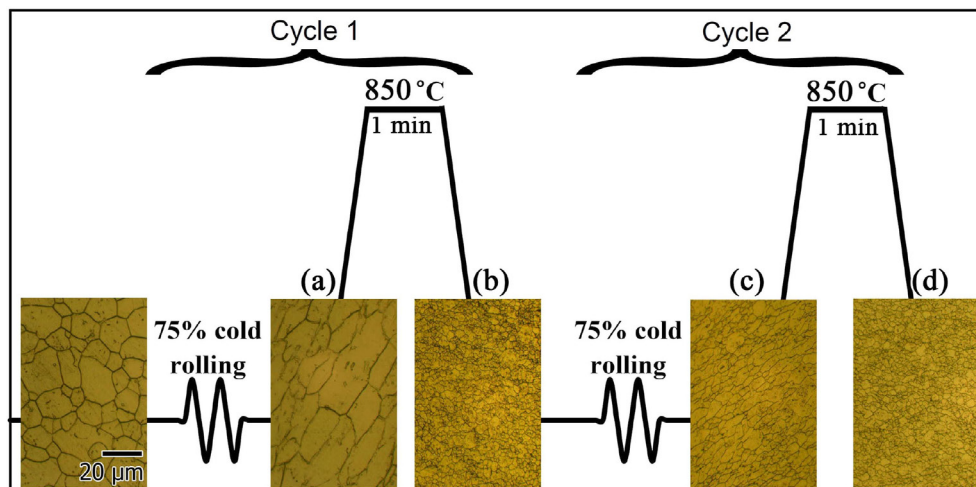


Fig. 5- (a) The 75% cold rolled AISI 304L stainless steel sample, (b) The annealed sample at 850 °C for 1 min, (c) The repetition of the 75% cold rolling, and (d) The repetition of the annealing at 850 °C for 1 min [65].

Other variants of rolling such as asymmetric cold rolling [16], cross rolling [16,48], and repetitive corrugation and straightening by rolling (RCSR) [66] have been also used. For instance, the improvement of the mechanical properties of AISI 304 stainless steel by the combined RCSR and annealing process has been reported by Asghari-Rad et al. [66].

**4. Stages of reversion annealing and the underlying mechanisms**

Based on an experimental and thermodynamics study, Sohrabi et al. [67] showed that the formation and reversion of the strain-induced martensite can be rationalized based on the presence of ferrite

phase at equilibrium condition, which explains the metastability of the material. Accordingly, the saturation of the amount of martensite after annealing at moderate temperatures was unraveled as shown in Figure 6a for the AISI 304L stainless steel. The figure clearly shows the presence of saturation in the martensite content at each temperature, where the volume fraction of martensite at the saturation point and the required time decrease with increasing temperature. For instance, while at 715 °C, a complete reversion was achieved at 5400 s, ~ 8 vol% martensite was achieved after 7200 s at 700 °C and remained even after long holding time of 43200 s [67].

Figure 6b shows the calculated equilibrium

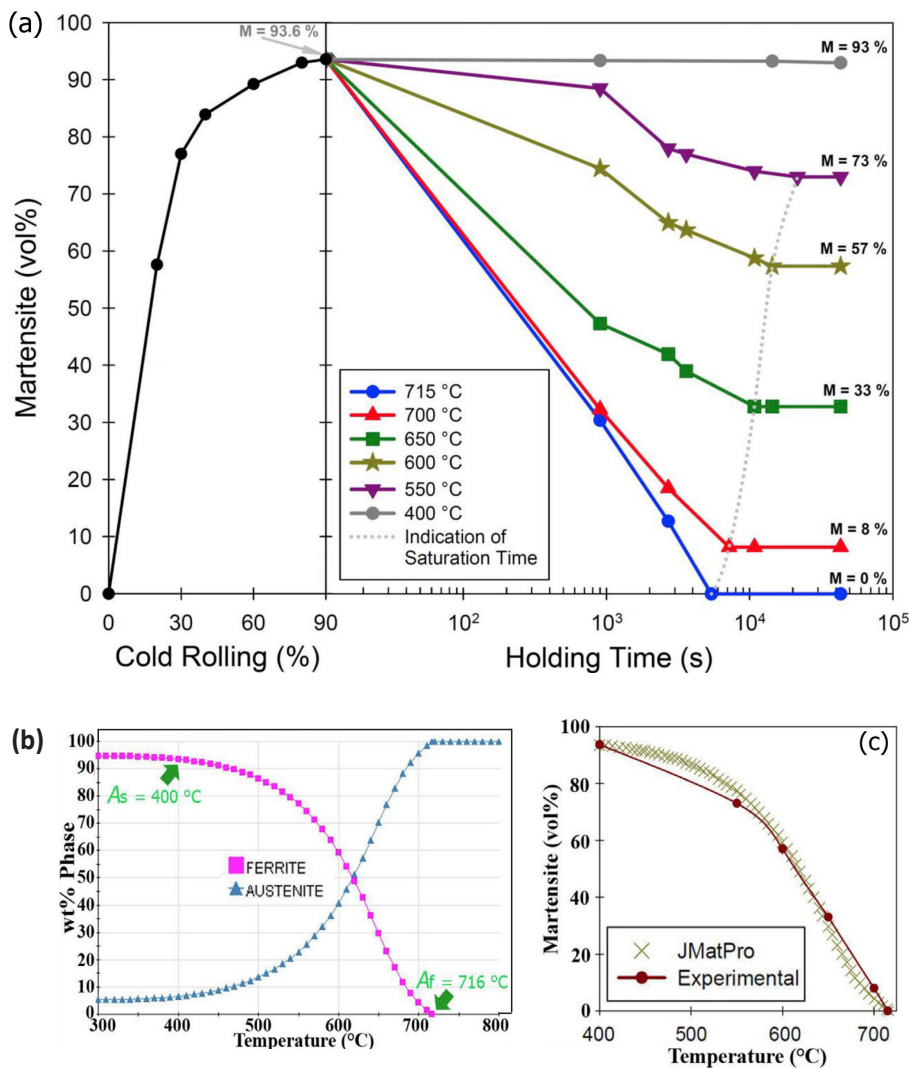


Fig. 6- (a) Formation and reversion of martensite in AISI 304L stainless steel, (b) calculated phases in AISI 304L stainless steel by JMatPro, and (c) comparison of JMatPro predictions with the experimental data [67].

phases versus temperature for the AISI 304L alloy. The experimental saturated martensite contents (Figure 6a) and the predicted ferrite phase at each temperature based on the JMatPro analysis (Figure 6b) are compared in Figure 6c, where a good agreement can be seen.

Two principal mechanisms have been proposed for the reversion of martensite to austenite: diffusional-type and martensitic shear-type [12,25,33,51,68-71]. Diffusional reversion proceeds by the growth of austenite nucleated in the matrix. During cold deformation, the metastable austenite transforms to lath martensite, and after reversion, the stratum structure of austenite laths and blocks develops. However, at high strains, the lath martensitic structure is replaced by a dislocation cell structure with high dislocation density, and after reversion, a structure of fine equiaxed grains develops [69]. The martensitic shear reversion occurs during heating, which is followed by the continuous recrystallization of the highly dislocated reversed austenite [24,69,70]. In the obtained microstructures, the shear reversion is frequently characterized by elongated reversed grains with relatively higher dislocation densities [72]. Reversion mechanism mainly depends on the chemical composition of the material, the annealing temperature, and the heating rate [68]. A lower Ni/Cr ratio leads to increase in the austenitization temperature for the martensitic shear reversion, where at very low Ni/Cr ratio, the martensitic shear reversion can no longer occur. The critical driving force required for the complete martensitic shear reversion is  $\sim -500$  J/mol. The Gibbs free energy difference between BCC and FCC structures ( $\Delta G^{\alpha \rightarrow \gamma}$  in J/mol) can be calculated by Equation 1 [68,71]:

$$\Delta G^{\alpha \rightarrow \gamma}(\text{J/mol}) = 10^{-2} \Delta G_{Fe}^{\alpha \rightarrow \gamma} (100 - \text{Cr} - \text{Ni}) - 97.5 \text{Cr} - 2.02 \text{Cr}^2 - 108.8 \text{Ni} + 0.52 \text{Ni}^2 - 0.05 \text{CrNi} + 10^{-3} T (73.3 \text{Cr} - 0.67 \text{Cr}^2 + 50.2 \text{Ni} - 0.84 \text{Ni}^2 - 1.51 \text{CrNi}) \quad (1)$$

where  $\Delta G_{Fe}^{\alpha \rightarrow \gamma}$  is the Gibbs free energy difference between BCC and FCC structures in pure iron [2,71], T is the absolute temperature in Kelvin, and the alloying elements have been expressed in mass percent. When  $\Delta G^{\alpha \rightarrow \gamma}$  is less than -500 J/mol, the martensitic shear reversion can occur completely [68]. Since the commercial alloys have elements other than Cr and Ni, the effects of alloying elements can be taken into account based on the relations proposed for the  $\text{Cr}_{eq}$  and  $\text{Ni}_{eq}$ . The

commonly used expressions are as follows [33]:

$$\begin{aligned} \text{Cr}_{eq} &= \text{Cr} + 4.5 \text{Mo} \\ \text{Ni}_{eq} &= \text{Ni} + 0.6 \text{Mn} + 20 \text{C} + 4 \text{N} - 0.4 \text{Si} \end{aligned} \quad (2)$$

The concept of incorporating the  $\text{Cr}_{eq}$  and  $\text{Ni}_{eq}$  values into the  $\Delta G^{\alpha \rightarrow \gamma}$  has been successfully used for studying the reversion mechanism by Iranian scientists [51,73,74]. It was considered by Shirdel et al. [51] for an AISI 304L stainless steel, where the expressions for the  $\text{Cr}_{eq}$  and  $\text{Ni}_{eq}$  were revised to include other alloying elements as shown in Equation 3 [51]:

$$\begin{aligned} \text{Cr}_{eq} &= \text{Cr} + 2 \text{Si} + 1.5 \text{Mo} + 5 \text{V} + 5.5 \text{Al} + 1.75 \text{Nb} + 1.5 \text{Ti} + 0.75 \text{W} \\ \text{Ni}_{eq} &= \text{Ni} + \text{Co} + 0.5 \text{Mn} + 0.3 \text{Cu} + 25 \text{N} + 30 \text{C} \end{aligned} \quad (3)$$

The results are summarized in Figure 7, where this figure indicates that the shear reversion is predominant above the estimated temperature of 783 °C for AISI 304L stainless steel. Similarly, Sabooni et al. [73] and Moallemi et al. [74] used the concept of  $\text{Cr}_{eq}$  and  $\text{Ni}_{eq}$  for investigating the reversion mechanism.

The different stages of microstructural evolution during annealing of cold rolled austenitic stainless steel were systematically studied by Naghizadeh and Mirzadeh [41,75] and Kheiri et al. [42], which enable microstructural control during thermomechanical processing. During reversion annealing, the reversion of strain-induced martensite to austenite, the primary recrystallization of the retained austenite (if it is present), and the grain growth process are important phenomena [2,31,32,41,42,75-78], which significantly affect the resultant microstructure and mechanical properties as discussed in the following for the AISI 316L stainless steel.

The evolution of the hardness of the cold-rolled AISI 316L stainless steel with a microstructure comprising of martensite and 22 vol% retained austenite during annealing is shown in Figure 8 [42]. It can be seen that at each temperature, hardness decreases by increasing holding time. Moreover, firstly this decrease is more pronounced (first stage), but then, the rate of hardness change decreases considerably in the second stage. However, for the high annealing temperature of 1050 °C, the decrease of hardness in the second stage is much more pronounced. Furthermore, as the temperature increases, the overall level of hardness

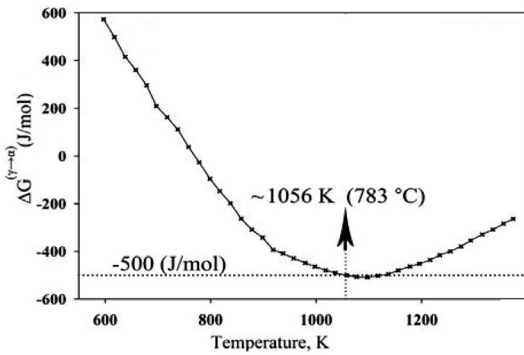


Fig. 7- Gibbs free energy change versus temperature for AISI 304L stainless steel [51].

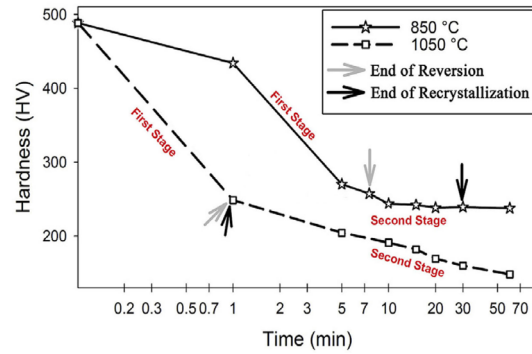


Fig. 8- Evolution of hardness of cold-rolled AISI 316L stainless steel during annealing [42].

declines. Figure 9 depicts the corresponding microstructural evolutions.

By annealing the cold rolled sample (Figure 9a) for 1 min at 850 °C, some dark regions appear in the microstructure (Figure 9b), which contain ultrafine reversed austenite grains (Figure 9c). For 7.5 min at 850 °C, fine grains occupy the majority of the microstructure, but some remained deformed regions are still available (Figure 9d). However, the corresponding XRD pattern (Figure 9e) reveals that the reversion process has been already completed at this stage. Therefore, the remaining deformed regions are the unrecrystallized austenite grains. Hence, longer holding durations at 850 °C are required to obtain a fully recrystallized microstructure, which was realized at holding time of 30 min at 850 °C as can be observed in Figures 9f and 9g. Further annealing does not considerably change the microstructure due to the sluggish grain growth at 850 °C (Figure 9h). For the annealing temperature of 1050 °C, a fully recrystallized microstructure was obtained after 1 min annealing (Figures 9i and 9j). Continued annealing up to 30 min results in significant grain growth as shown in Figure 9k [42]. The latter can be related to the temperature-dependency of the pinning effect of Mo, where the concentration of the solute Mo atoms in the boundaries decreases by increasing temperature [79].

The kinetics of phase transformations during annealing of the cold rolled AISI 309Si stainless steel was investigated by Abdi et al. [77], where the reverse transformation of martensite and recrystallization of the retained austenite were separated. The kinetics analysis revealed that the activation energy of both processes is equal to the lattice diffusion activation energy in

austenitic stainless steels [80]. Consequently, the recrystallization–temperature–time diagram of the alloy was devised as shown in Figure 10.

A two-step annealing treatment after cold rolling was proposed by Sharifian et al. [78] for the optimization of the annealing process of AISI 316L austenitic stainless steel toward better grain refinement. The first step of the annealing process at lower temperatures was used for the reversion of strain-induced martensite to austenite without uninhibited grain growth and recrystallization of the retained austenite. Afterwards, the primary recrystallization of the retained austenite takes place in the second step of the annealing process at higher temperatures. Carefully controlling the second annealing step resulted in a finer grain size and better mechanical response compared to those of a conventional one-step annealing approach [78].

### 5. TRIP effect

The formation of martensite during deformation is responsible for the enhanced work-hardening rate, the inhibition of necking, and increased uniform elongation [13]. This is known as the TRIP effect and plays a major role in determining the mechanical properties of metastable austenitic stainless steels [2,13,19,22,42,43,46,51,75,81]. For the reversion-treated austenitic Fe-Cr-Ni stainless steels, the TRIP effect has been investigated extensively by Mirzadeh and coworkers [42,43,51,75]. Firstly, Shirdel et al. [51] showed that grain refinement results in a less pronounced TRIP effect in AISI 304L stainless steel. Subsequently, this effect was thoroughly studied by Naghizadeh and Mirzadeh [75], where the summary of mechanical properties of reversion-treated AISI 304 stainless

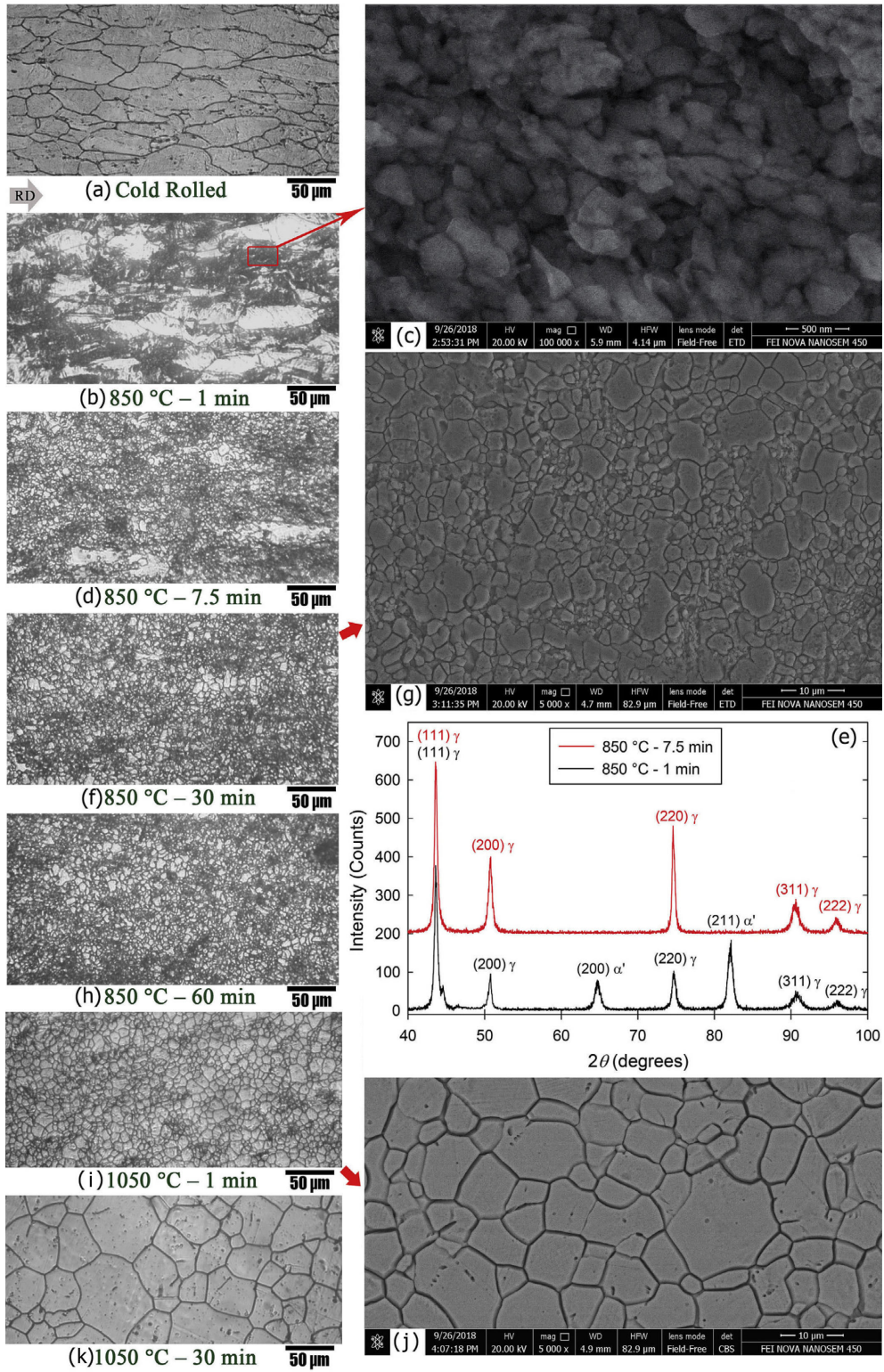


Fig. 9- Obtained microstructures and XRD patterns after reversion annealing of the cold-rolled AISI 316L stainless steel [42].

steel is shown in Figure 11.

Figure 11a reveals that grain refinement significantly enhances the yield stress (YS) and ultimate tensile strength (UTS) of the material while decreases the total elongation. The effect of grain size on the YS is much more pronounced as shown in Figure 11b, which is related to the dependency of UTS on the grain size dependent TRIP effect. The lower Hall-Petch slope for the UTS ( $166 \text{ MPa}\cdot\mu\text{m}^{0.5}$ ) compared to that of YS ( $391 \text{ MPa}\cdot\mu\text{m}^{0.5}$ ) implies a lower grain size dependency for the former due to the TRIP effect. Since the stability of the austenite phase normally increases with refining grain size, the TRIP effect becomes less dominant in the fine-grained austenite, and hence, the increase in the tensile strength becomes less significant due to the deterioration of the work-hardening capacity as shown in Figures 11c and 11d [75].

The mechanical properties of UFG Fe-Cr-Ni austenitic stainless steels have been also extensively studied by the Iranian scientists. For instance, Table 1 summarizes the obtained tensile properties after reversion annealing for the AISI 304L stainless steel in some of the reported Iranian works. It can be

seen that the YS, UTS, and total elongation are in the ranges of 720 to 1100 MPa, 920 to 1200 MPa, and 40 to 47%, respectively. The table reveals that the average grain sizes below  $0.5 \mu\text{m}$  ( $500 \text{ nm}$ ) are favorable for increasing the yield stress, but deteriorate the work hardening behavior (as can be evaluated by the value of  $\text{UTS}-\text{YS}$ ). Moreover,

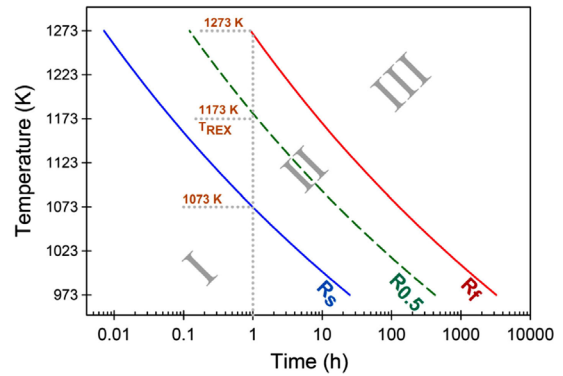


Fig.10- Recrystallization-temperature-time diagram of 90% cold-rolled AISI 309Si stainless steel [77].  $R_s$ ,  $R_{0.5}$ , and  $R_f$  represent the recrystallization start, 50% recrystallization, and the recrystallization finish, respectively.  $T_{\text{REX}}$  represents the recrystallization temperature.

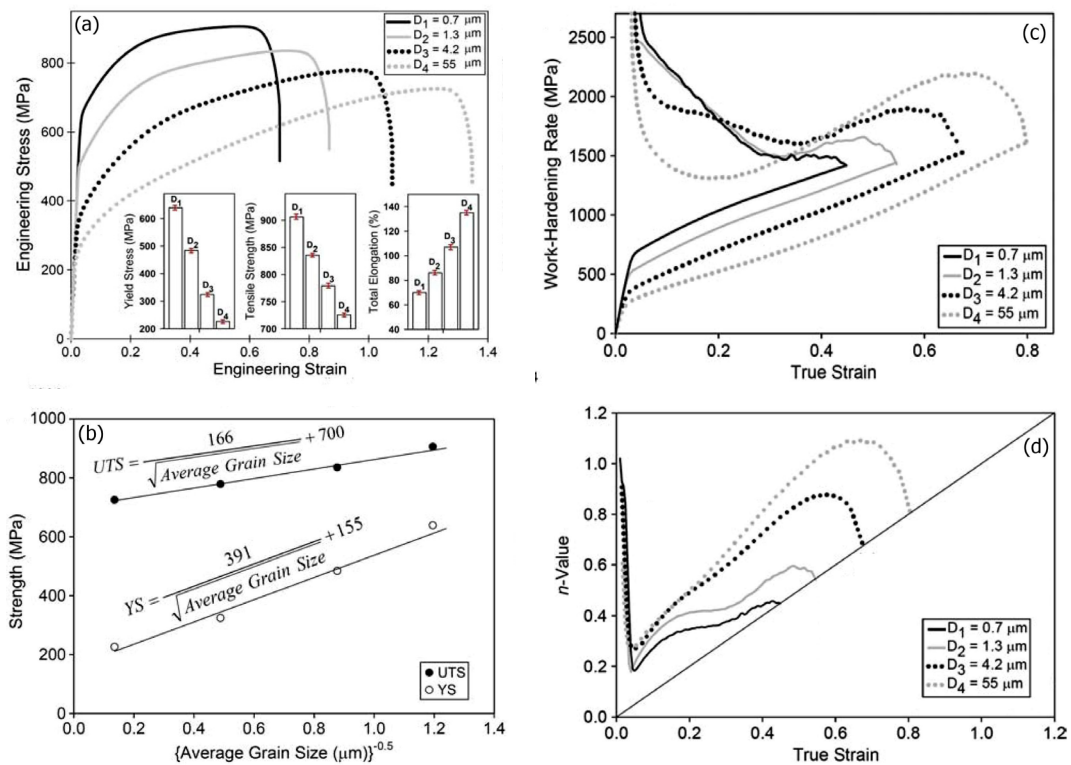


Fig. 11- Summary of mechanical properties of reversion-treated AISI 304 stainless steel [75].

Table 1- Tensile properties of reversion annealed AISI 304L stainless steels

YS (MPa)	UTS (MPa)	Total elongation (%)	Average grain size ( $\mu\text{m}$ )	Reference
1100	1200	46	0.40	[43]
855	1385	44	0.62	[51]
1000	1010	40	0.33	[53]
720	920	47	0.65	[62]

the mechanical properties depend on the details of the reversion annealing treatment. For instance, the remarkable mechanical properties reported by Sohrabi et al. [43] have been obtained by continuous heating of the cold rolled sheet from room temperature to 750 °C at the heating rate of 5 °C/min.

Distinct Lüders-like deformation has been found recently in the steels having austenite matrix or retained austenite, where the Lüders elongation usually accounted for more than half of the total elongation of the material [24,43,82,83]. It has been also demonstrated that the remarkable Lüders-type deformation is closely associated with the deformation-induced martensitic transformation occurring in the band region with high localized plastic strain. The early plastic instability just after yielding is a characteristic of UFG metals, which originates from the nature of limited strain hardening capability in the UFG microstructures. Such early plastic instability usually leads to a quick tensile failure. However, in UFG austenitic stainless steels, the strain-induced martensitic transformation can be triggered once a critical plastic strain is achieved in the necked region (band region), which in turn provides extra-strain hardening and helps resisting further strain localization [83]. The discontinuous yielding phenomenon in AISI 301LN stainless steel has been also connected to the effective grain size refinement or/and precipitation [24,29,84]. Moreover, for a AISI 301LN stainless steel (cryorolled and annealed at 750 °C for 30 min), the discontinuous yielding has been partly correlated to the relative flow stress difference between work hardened fine-grained austenite and deformation-induced martensite, resulting in a negative strain hardening rate contribution balancing the influence of the work hardening of austenite [85].

The Lüders-type deformation has been observed by Sohrabi et al [43] for a reversion-treated AISI 304L stainless steel while it was not observed for the reversion-treated AISI 316L stainless steel. This can be related to the difference in the grain size, where the average grain size of the former and

the latter alloys was obtained as 0.4 and 2.3  $\mu\text{m}$ , respectively. In fact, the equiaxed microstructure of the AISI 316L stainless steel was achieved after recrystallization of the retained austenite and some grain growth of the reversed grains, which resulted in a much larger grain size compared to that obtained for the AISI 304L stainless steel. The inhibition of the recrystallization in the AISI 316L stainless steel was explained by the retardation effect of alloying elements (molybdenum in this case), which postpones the formation of the equiaxed structure, and hence, greatly affects the obtainable grain size and the resultant mechanical properties [43].

## 6. Summary

The notable contributions of Iranian scientists in the field of formation and reversion of strain-induced martensite for grain refinement and enhanced mechanical properties of Fe-Cr-Ni austenitic stainless steels are reviewed. The following conclusions can be drawn:

(1) The processing of ultrafine grained (UFG) structure in Fe-Cr-Ni austenitic stainless steels via cold rolling and reversion annealing was summarized. The repetitive and innovative thermomechanical processing routes were introduced as well. The published research works include a majority of the commercially available Fe-Cr-Ni austenitic stainless steels. However, as preliminary evaluated recently, it is expected that the addition of microalloying elements and Mn- and N-containing alloys (with reduced amounts of Ni) gain more attention in the future for the purpose of reduction of the processing cost and lowering the required cold reduction for processing of the UFG structure.

(2) The annealing-induced martensite formation due to carbide formation and local decrease in the martensite start temperature has been observed by Iranian scientists. Moreover, the corrosion resistance and wear behavior of the reversion-treated austenitic stainless steels have been briefly studied. Investigation of mechanical response beyond tensile and hardness tests has not

been considered properly, including fatigue and formability. These subjects deserve more systematic investigations.

(3) The understanding of the stages of annealing (reversion of strain-induced martensite to austenite, primary recrystallization of the retained austenite, and grain growth) and the underlying reversion mechanisms (diffusional-type and martensitic shear-type) constituted the subsequent part of this overview. The importance of the retained austenite on the obtainable grain size of the reversion-treated austenitic stainless steels was discussed.

(4) The TRIP effect in the reversion-treated metastable austenitic stainless steels was discussed. It was revealed that the grain refinement results in a less pronounced TRIP effect. The remarkable Lüders-type deformation in the UFG austenitic stainless steels is a hot topic in the world and needs to be studied in future by Iranian scientists. In fact, the Lüders elongation might account for more than half of the total elongation of the materials. Thus, the Lüders-like deformation is considered to play a key role for obtaining the excellent mechanical properties with both high strength and large tensile ductility.

## References

1. Karjalainen LP, Taulavuori T, Sellman M, Kyröläinen A. Some Strengthening Methods for Austenitic Stainless Steels. *steel research international*. 2008;79(6):404-12.
2. Sohrabi MJ, Naghizadeh M, Mirzadeh H. Deformation-induced martensite in austenitic stainless steels: A review. *Archives of Civil and Mechanical Engineering*. 2020;20(4).
3. Maki T. Stainless steel: progress in thermomechanical treatment. *Current Opinion in Solid State and Materials Science*. 1997;2(3):290-5.
4. Talonen J, Hänninen H. Formation of shear bands and strain-induced martensite during plastic deformation of metastable austenitic stainless steels. *Acta Materialia*. 2007;55(18):6108-18.
5. Padilha AF, Plaut RL, Rios PR. Annealing of Cold-worked Austenitic Stainless Steels. *ISIJ International*. 2003;43(2):135-43.
6. Mehranfar M, Dehghani K. Producing nanostructured super-austenitic steels by friction stir processing. *Materials Science and Engineering: A*. 2011;528(9):3404-8.
7. Mohammad Nejad Fard N, Mirzadeh H, Mohammad R, Cabrera JM. Accumulative roll bonding of aluminum/stainless steel sheets. *Journal of Ultrafine Grained and Nanostructured Materials*. 2017 Jun 1;50(1):1-5.
8. Salvatori I, Inoue T, Nagai K. Ultrafine Grain Structure through Dynamic Recrystallization for Type 304 Stainless Steel. *ISIJ International*. 2002;42(7):744-50.
9. Souza RC, Silva ES, Jorge AM, Cabrera JM, Balancin O. Dynamic recovery and dynamic recrystallization competition on a Nb- and N-bearing austenitic stainless steel biomaterial: Influence of strain rate and temperature. *Materials Science and Engineering: A*. 2013;582:96-107.
10. Mirzadeh H, Cabrera JM, Najafizadeh A, Calvillo PR. EBSD study of a hot deformed austenitic stainless steel. *Materials Science and Engineering: A*. 2012;538:236-45.
11. Dehghan-Manshadi A, Barnett MR, Hodgson PD. Recrystallization in AISI 304 austenitic stainless steel during and after hot deformation. *Materials Science and Engineering: A*. 2008;485(1-2):664-72.
12. Tomimura K, Takaki S, Tanimoto S, Tokunaga Y. Optimal Chemical Composition in Fe-Cr-Ni Alloys for Ultra Grain Refining by Reversion from Deformation Induced Martensite. *ISIJ International*. 1991;31(7):721-7.
13. Soleimani M, Kalhor A, Mirzadeh H. Transformation-induced plasticity (TRIP) in advanced steels: A review. *Materials Science and Engineering: A*. 2020;795:140023.
14. Zergani A, Mirzadeh H, Mahmudi R. Evolutions of mechanical properties of AISI 304L stainless steel under shear loading. *Materials Science and Engineering: A*. 2020;791:139667.
15. Eskandari M, Zarei-Hanzaki A, Abedi HR. An investigation into the room temperature mechanical properties of nanocrystalline austenitic stainless steels. *Materials & Design*. 2013;45:674-81.
16. Amininejad A, Jamaati R, Hosseinipour SJ. Improvement of strength-ductility balance of SAE 304 stainless steel by asymmetric cross rolling. *Materials Chemistry and Physics*. 2020;256:123668.
17. Shirdel M, Mirzadeh H, Parsa MH. Estimation of the kinetics of martensitic transformation in austenitic stainless steels by conventional and novel approaches. *Materials Science and Engineering: A*. 2015;624:256-60.
18. Mirzaie T, Mirzadeh H, Naghizadeh M. Contribution of Different Hardening Mechanisms during Cold Working of AISI 304L Austenitic Stainless Steel. *Archives of Metallurgy and Materials*. 2018;63.
19. Zergani A, Mirzadeh H, Mahmudi R. Unraveling the Effect of Deformation Temperature on the Mechanical Behavior and Transformation-Induced Plasticity of the SUS304L Stainless Steel. *steel research international*. 2020;91(9):2000114.
20. Lo KH, Shek CH, Lai JKL. Recent developments in stainless steels. *Materials Science and Engineering: R: Reports*. 2009;65(4-6):39-104.
21. Olson GB, Cohen M. Kinetics of strain-induced martensitic nucleation. *Metallurgical Transactions A*. 1975;6(4):791-5.
22. Hamada AS, Karjalainen LP, Misra RDK, Talonen J. Contribution of deformation mechanisms to strength and ductility in two Cr-Mn grade austenitic stainless steels. *Materials Science and Engineering: A*. 2013;559:336-44.
23. Naghizadeh M, Mirzadeh H. Modeling the kinetics of deformation-induced martensitic transformation in AISI 316 metastable austenitic stainless steel. *Vacuum*. 2018;157:243-8.
24. Järvenpää A, Jaskari M, Kisko A, Karjalainen P. Processing and Properties of Reversion-Treated Austenitic Stainless Steels. *Metals*. 2020;10(2):281.
25. Behjati P, Kermanpur A, Najafizadeh A. Application of Martensitic Transformation Fundamentals to Select Appropriate Alloys for Grain Refining Through Martensite Thermomechanical Treatment. *Metallurgical and Materials Transactions A*. 2013;44(8):3524-31.
26. Parnian P, Parsa MH, Mirzadeh H, Jafarian HR. Effect of Drawing Strain on Development of Martensitic Transformation and Mechanical Properties in AISI 304L Stainless Steel Wire. *steel research international*. 2017;88(8):1600423.
27. Kisko A, Misra RDK, Talonen J, Karjalainen LP. The influence of grain size on the strain-induced martensite formation in tensile straining of an austenitic 15Cr-9Mn-Ni-Cu stainless steel. *Materials Science and Engineering: A*. 2013;578:408-16.
28. Souza Filho IR, Sandim MJR, Cohen R, Nagamine LCCM, Hoffmann J, Bolmaro RE, et al. Effects of strain-induced

- martensite and its reversion on the magnetic properties of AISI 201 austenitic stainless steel. *Journal of Magnetism and Magnetic Materials*. 2016;419:156-65.
29. Järvenpää A, Jaskari M, Karjalainen L. Reversed Microstructures and Tensile Properties after Various Cold Rolling Reductions in AISI 301LN Steel. *Metals*. 2018;8(2):109.
30. Xu DM, Li GQ, Wan XL, Misra RDK, Zhang XG, Xu G, et al. The effect of annealing on the microstructural evolution and mechanical properties in phase reversed 316LN austenitic stainless steel. *Materials Science and Engineering: A*. 2018;720:36-48.
31. Kisko A, Hamada AS, Talonen J, Porter D, Karjalainen LP. Effects of reversion and recrystallization on microstructure and mechanical properties of Nb-alloyed low-Ni high-Mn austenitic stainless steels. *Materials Science and Engineering: A*. 2016;657:359-70.
32. Sun GS, Du LX, Hu J, Misra RDK. Microstructural evolution and recrystallization behavior of cold rolled austenitic stainless steel with dual phase microstructure during isothermal annealing. *Materials Science and Engineering: A*. 2018;709:254-64.
33. Somani MC, Juntunen P, Karjalainen LP, Misra RDK, Kyröläinen A. Enhanced Mechanical Properties through Reversion in Metastable Austenitic Stainless Steels. *Metallurgical and Materials Transactions A*. 2009;40(3):729-44.
34. Schino AD, Salvatori I, Kenny JM. Effects of martensite formation and austenite reversion on grain refining of AISI 304 stainless steel. *Journal of Materials Science*. 2002 Nov 1;37(21):4561-5.
35. Li J, Cao Y, Gao B, Li Y, Zhu Y. Superior strength and ductility of 316L stainless steel with heterogeneous lamella structure. *Journal of Materials Science*. 2018;53(14):10442-56.
36. Li J, Gao B, Huang Z, Zhou H, Mao Q, Li Y. Design for strength-ductility synergy of 316L stainless steel with heterogeneous lamella structure through medium cold rolling and annealing. *Vacuum*. 2018;157:128-35.
37. Wang S, Li J, Cao Y, Gao B, Mao Q, Li Y. Thermal stability and tensile property of 316L stainless steel with heterogeneous lamella structure. *Vacuum*. 2018;152:261-4.
38. Mirzadeh H, Najafzadeh A. Correlation between processing parameters and strain-induced martensitic transformation in cold worked AISI 301 stainless steel. *Materials Characterization*. 2008;59(11):1650-4.
39. Mirzadeh H, Najafzadeh A. ANN modeling of strain-induced martensite and its applications in metastable austenitic stainless steels. *Journal of Alloys and Compounds*. 2009;476(1-2):352-5.
40. Mirzadeh H, Najafzadeh A. Modeling the reversion of martensite in the cold worked AISI 304 stainless steel by artificial neural networks. *Materials & Design*. 2009;30(3):570-3.
41. Naghizadeh M, Mirzadeh H. Microstructural Evolutions During Annealing of Plastically Deformed AISI 304 Austenitic Stainless Steel: Martensite Reversion, Grain Refinement, Recrystallization, and Grain Growth. *Metallurgical and Materials Transactions A*. 2016;47(8):4210-6.
42. Kheiri S, Mirzadeh H, Naghizadeh M. Tailoring the microstructure and mechanical properties of AISI 316L austenitic stainless steel via cold rolling and reversion annealing. *Materials Science and Engineering: A*. 2019;759:90-6.
43. Sohrabi MJ, Mirzadeh H, Dehghanian C. Significance of Martensite Reversion and Austenite Stability to the Mechanical Properties and Transformation-Induced Plasticity Effect of Austenitic Stainless Steels. *Journal of Materials Engineering and Performance*. 2020;29(5):3233-42.
44. Shirdel M, Mirzadeh H, Parsa MH. Enhanced Mechanical Properties of Microalloyed Austenitic Stainless Steel Produced by Martensite Treatment. *Advanced Engineering Materials*. 2015;17(8):1226-33.
45. Sadeghpour S, Kermanpur A, Najafzadeh A. Influence of Ti microalloying on the formation of nanocrystalline structure in the 201L austenitic stainless steel during martensite thermomechanical treatment. *Materials Science and Engineering: A*. 2013;584:177-83.
46. Behjati P, Kermanpur A, Najafzadeh A, Samaei Baghbadorani H, Karjalainen LP, Jung JG, et al. Design of a new Ni-free austenitic stainless steel with unique ultrahigh strength-high ductility synergy. *Materials & Design*. 2014;63:500-7.
47. Moallemi M, Kermanpur A, Najafzadeh A, Rezaee A, Samaei baghbadorani H. Formation of nano/ultrafine grain structure in a 201 stainless steel through the repetitive martensite thermomechanical treatment. *Materials Letters*. 2012;89:22-4.
48. Eskandari M, Kermanpur A, Najafzadeh A. Formation of Nanocrystalline Structure in 301 Stainless Steel Produced by Martensite Treatment. *Metallurgical and Materials Transactions A*. 2009;40(9):2241-9.
49. Johannsen DL, Kyrolainen A, Ferreira PJ. Influence of annealing treatment on the formation of nano/submicron grain size AISI 301 Austenitic stainless steels. *Metallurgical and Materials Transactions A*. 2006;37(8):2325-38.
50. Gauzzi F, Montanari R, Principi G, Tata ME. AISI 304 steel: anomalous evolution of martensitic phase following heat treatments at 400°C. *Materials Science and Engineering: A*. 2006;438-440:202-6.
51. Shirdel M, Mirzadeh H, Parsa MH. Nano/ultrafine grained austenitic stainless steel through the formation and reversion of deformation-induced martensite: Mechanisms, microstructures, mechanical properties, and TRIP effect. *Materials Characterization*. 2015;103:150-61.
52. Zhou Z, Wang S, Li J, Li Y, Wu X, Zhu Y. Hardening after annealing in nanostructured 316L stainless steel. *Nano Materials Science*. 2020;2(1):80-2.
53. Forouzan F, Najafzadeh A, Kermanpur A, Hedayati A, Surkialliabad R. Production of nano/submicron grained AISI 304L stainless steel through the martensite reversion process. *Materials Science and Engineering: A*. 2010;527(27-28):7334-9.
54. Shahri MG, Hosseini SR, Salehi M. Formation of Nano/Ultrafine Grains in AISI 321 Stainless Steel Using Advanced Thermo-Mechanical Process. *Acta Metallurgica Sinica (English Letters)*. 2015;28(4):499-504.
55. Rezaei HA, Ghazani MS, Eghbali B. Effect of post deformation annealing on the microstructure and mechanical properties of cold rolled AISI 321 austenitic stainless steel. *Materials Science and Engineering: A*. 2018;736:364-74.
56. Bakhsheshi-Rad HR, Haerian B, Najafzadeh A, Idris MH, Kadir MRA, Hamzah E, et al. Cold deformation and heat treatment influence on the microstructures and corrosion behavior of AISI 304 stainless steel. *Canadian Metallurgical Quarterly*. 2013;52(4):449-57.
57. Sohrabi MJ, Mirzadeh H, Dehghanian C. Unraveling the effects of surface preparation on the pitting corrosion resistance of austenitic stainless steel. *Archives of Civil and Mechanical Engineering*. 2020;20(1).
58. Sabooni S, Rashtchi H, Eslami A, Karimzadeh F, Enayati MH, Raeissi K, et al. Dependence of corrosion properties of AISI 304L stainless steel on the austenite grain size. *International Journal of Materials Research*. 2017;108(7):552-9.
59. Nafar Dehsorkhi R, Sabooni S, Karimzadeh F, Rezaeian A, Enayati MH. The effect of grain size and martensitic transformation on the wear behavior of AISI 304L stainless steel. *Materials & Design*. 2014;64:56-62.

60. Shirdel M, Mirzadeh H, Parsa MH. Abnormal grain growth in AISI 304L stainless steel. *Materials Characterization*. 2014;97:11-7.
61. Shirdel M, Mirzadeh H, Habibi Parsa M. Microstructural Evolution During Normal/Abnormal Grain Growth in Austenitic Stainless Steel. *Metallurgical and Materials Transactions A*. 2014;45(11):5185-93.
62. Sabooni S, Karimzadeh F, Enayati MH. Thermal Stability Study of Ultrafine Grained 304L Stainless Steel Produced by Martensitic Process. *Journal of Materials Engineering and Performance*. 2014;23(5):1665-72.
63. Ma Y, Jin J, Lee Y. A repetitive thermomechanical process to produce nano-crystalline in a metastable austenitic steel. *Scripta Materialia*. 2005;52(12):1311-5.
64. Momeni A, Abbasi SM. Repetitive Thermomechanical Processing towards Ultra Fine Grain Structure in 301, 304 and 304L Stainless Steels. *Journal of Materials Science & Technology*. 2011;27(4):338-43.
65. Naghizadeh M, Mirzadeh H. Processing of fine grained AISI 304L austenitic stainless steel by cold rolling and high-temperature short-term annealing. *Materials Research Express*. 2018;5(5):056529.
66. Asghari-Rad P, Nili-Ahmadabadi M, Shirazi H, Hossein Nedjad S, Koldorf S. A Significant Improvement in the Mechanical Properties of AISI 304 Stainless Steel by a Combined RCSR and Annealing Process. *Advanced Engineering Materials*. 2017;19(3):1600663.
67. Sohrabi MJ, Mirzadeh H, Dehghanian C. Thermodynamics basis of saturation of martensite content during reversion annealing of cold rolled metastable austenitic steel. *Vacuum*. 2020;174:109220.
68. Tomimura K, Takaki S, Tokunaga Y. Reversion Mechanism from Deformation Induced Martensite to Austenite in Metastable Austenitic Stainless Steels. *ISIJ International*. 1991;31(12):1431-7.
69. Takaki S, Tomimura K, Ueda S. Effect of Pre-cold-working on Diffusional Reversion of Deformation Induced Martensite in Metastable Austenitic Stainless Steel. *ISIJ International*. 1994;34(6):522-7.
70. Misra RDK, Nayak S, Venkatasurya PKC, Ramuni V, Somani MC, Karjalainen LP. Nanograined/Ultrafine-Grained Structure and Tensile Deformation Behavior of Shear Phase Reversion-Induced 301 Austenitic Stainless Steel. *Metallurgical and Materials Transactions A*. 2010;41(8):2162-74.
71. Nasiri Z, Ghaemifar S, Naghizadeh M, Mirzadeh H. Thermal Mechanisms of Grain Refinement in Steels: A Review. *Metals and Materials International*. 2020.
72. Shakhova I, Dudko V, Belyakov A, Tsuzaki K, Kaibyshev R. Effect of large strain cold rolling and subsequent annealing on microstructure and mechanical properties of an austenitic stainless steel. *Materials Science and Engineering: A*. 2012;545:176-86.
73. Sabooni S, Karimzadeh F, Enayati MH, Ngan AHW. The role of martensitic transformation on bimodal grain structure in ultrafine grained AISI 304L stainless steel. *Materials Science and Engineering: A*. 2015;636:221-30.
74. Moallemi M, Zarei-Hanzaki A, Kim S-J, Alimadadi H. On the microstructural-textural characterization and deformation analysis of a nano/ultrafine grained Fe-20Cr-8Mn-0.3N duplex alloy with superior mechanical properties. *Materials Characterization*. 2019;156:109878.
75. Naghizadeh M, Mirzadeh H. Microstructural Effects of Grain Size on Mechanical Properties and Work-Hardening Behavior of AISI 304 Austenitic Stainless Steel. *steel research international*. 2019;90(10):1900153.
76. Naghizadeh M, Mirzadeh H. Microstructural Evolutions During Reversion Annealing of Cold-Rolled AISI 316 Austenitic Stainless Steel. *Metallurgical and Materials Transactions A*. 2018;49(6):2248-56.
77. Abdi A, Mirzadeh H, Sohrabi MJ, Naghizadeh M. Phase Transformation Kinetics During Annealing of Cold-Rolled AISI 309Si Stainless Steel. *Metallurgical and Materials Transactions A*. 2020;51(5):1955-9.
78. Sharifian K, Mirzadeh H, Kheiri S, Naghizadeh M. Two-step annealing treatment for grain refinement of cold-worked AISI 316L stainless steel. *International Journal of Materials Research*. 2020;111(8):676-80.
79. Naghizadeh M, Mirzadeh H. Elucidating the Effect of Alloying Elements on the Behavior of Austenitic Stainless Steels at Elevated Temperatures. *Metallurgical and Materials Transactions A*. 2016;47(12):5698-703.
80. Mirzadeh H, Cabrera JM, Najafizadeh A. Constitutive relationships for hot deformation of austenite. *Acta Materialia*. 2011;59(16):6441-8.
81. Qin W, Li J, Liu Y, Kang J, Zhu L, Shu D, et al. Effects of grain size on tensile property and fracture morphology of 316L stainless steel. *Materials Letters*. 2019;254:116-9.
82. Li J, Zhou Z, Wang S, Mao Q, Fang C, Li Y, et al. Deformation mechanisms and enhanced mechanical properties of 304L stainless steel at liquid nitrogen temperature. *Materials Science and Engineering: A*. 2020;798:140133.
83. Gao S, Bai Y, Zheng R, Tian Y, Mao W, Shibata A, et al. Mechanism of huge Lüders-type deformation in ultrafine grained austenitic stainless steel. *Scripta Materialia*. 2019;159:28-32.
84. A. Järvenpää, Microstructures, Mechanical stability and strength of low-temperature AISILN stainless steel under monotonic and dynamic loading, Ph.D. Thesis, University of Oulu, Oulu, Finland, 2019.
85. D. Maréchal, Linkage between Mechanical Properties and Phase Transformations in a 301LN Austenitic Stainless Steel, Ph.D. Thesis, University of British Columbia, Vancouver, BC, Canada, 2011.